

# Geometry Optimization of the Side Coupled Structure used for the Fermilab Linac Upgrade

R. J. Noble and P. Zhou

*Fermi National Accelerator Laboratory\**

*P. O. Box 500, Batavia, Illinois 60510*

June 8, 1990

## Abstract

The Fermilab Linac Upgrade will replace the last four tanks of the 201.25 MHz drift-tube linac with 805 MHz side-coupled cavity modules to increase the final output energy from 200 Mev to 400 Mev. Physical restrictions, rf and beam dynamics considerations set strict requirements on the side-coupled cavities. It is desired to have a high effective shunt impedance for economy of rf power ( $ZT^2 \sim 45 M\Omega/m$ ) and a tolerably high surface electric field for reliable operation ( $\sim 1.4$  times the Kilpatrick limit). After extensive calculations using the computer code SUPERFISH to optimize the geometry for maximum  $ZT^2$  without exceeding a predetermined Kilpatrick limit, it was determined from high field experiments on a test model that the sparking level was excessive for reliable operation. Further changes were made to the geometry to reduce the surface field while only minimally effecting the shunt impedance.

---

\*Operated by the Universities Research Association under contract with the U. S. Department of Energy

## Introduction

Fermilab plans to upgrade the Tevatron to achieve higher luminosity so as to extend both the fixed target and collider operating modes. The first phase of this program is to increase the final kinetic energy of the  $H^-$  linac from 200 to 400 Mev<sup>[1]</sup>. This is expected to reduce the incoherent space-charge tuneshift at injection into the 8 GeV Booster which can limit either the brightness (particles per unit emittance) or the total intensity of the beam. The intended consequences of this will be to increase the collision rate in the antiproton-proton collider and the intensity for the fixed target experiments.

The present 200 MeV drift-tube linac (DTL) consists of nine accelerating cavities operating at a frequency of 201.25 MHz. The Linac Upgrade Project will replace the last four cavities, which accelerate the beam from 116 MeV to 200 MeV in a length of 66 m, with seven side-coupled cavity modules operating at a frequency of 805 MHz or four times the DTL frequency. The higher frequency allows higher accelerating gradients to be achieved so that a kinetic energy of 400 MeV can be reached in the same 66 m length. The 400 MeV energy is a maximum dictated by the fact that a higher energy  $H^-$  beam cannot be transported through the curved transfer line to the booster without stripping the electrons in the magnetic fields of the transport magnets. Each module will be driven with a klystron-based rf power supply rated to deliver a peak power of 12 MW. Purely from the standpoint of gradient, power economy and available sources, the choice of 805 MHz for the 400-MeV linac is toward the

low frequency side of a broad optimum. However, the longitudinal emittance of the beam from the 200 MHz linac is large enough that a larger frequency ratio between structures risks degrading the performance by nonlinearity of the phase-energy oscillations.

The side-coupled accelerating structure (SCS) was selected for the Fermilab Linac Upgrade because it is well understood and fully proven. This type of structure at 805 MHz was used on the LAMPF linac to accelerate the beam exiting the 201.25 MHz DTL from 100 Mev to 800 Mev. Since then the SCS has found its use in several high frequency electron accelerator devices.

## Design Assumptions and Criteria

The first and fundamental assumption in the upgrade program is that the side-coupled (SC) modules replacing the last four cavities should fit within the same length. Therefore, the average accelerating gradient  $E_0$  has to be about three times that of the DTL, or about 7.5 MV/m.

As can be seen from the relation  $ZT^2 = (E_0T)^2/(P/L)$ , where  $ZT^2$  is the effective shunt impedance,  $T$  the transit time factor and  $P/L$  the power per unit length, we have to increase the shunt impedance in order to reduce the power consumption. Klystrons producing tens of megawatts of peak power at several hundred megahertz are commercially available. If the structure dissipation is to be about 1 MW/m of peak power, then the structure shunt impedance must be about  $45M\Omega/m$  to achieve  $E_0 = 7.5MV/m$  when  $T \approx 0.9$ .

The coupling constant between accelerating and side cells is chosen to be approximately 5%. A 5% coupling slot will reduce the shunt impedance by about 12.5% relative to an unslotted cell. Larger couplings reduce the shunt impedance excessively. Smaller couplings lead to an excessive power flow amplitude droop, which is the change in field amplitude observed downstream from the rf drive port due to resistive wall losses, and phase shift in long chains of coupled accelerating cells<sup>[2]</sup>. For 5% coupling the amplitude droop  $\Delta A/A$  varies over the range of 0.3% to 0.2% and the power flow phase shift  $\Delta\phi$  varies over the range of  $0.6^\circ$  to  $0.5^\circ$  between the low and high energy ends of the side-coupled linac for the length of modules in the upgrade design. These deviations are considered acceptable because they are within the tolerances determined from beam dynamics considerations and control loops.

The maximum surface electric field occurring in an accelerator structure is determined by the limitations of voltage conditioning time, X-ray production and sparking rate. Sparking in linac cavities causes beam loss and beam intensity fluctuations in the downstream accelerators which deteriorates their performance. A tolerable sparking rate was set to be one spark per 1000 rf pulses in the new linac corresponding to less than 0.1% beam loss. Higher surface electric fields also produce more X-rays which will ultimately deteriorate the performance of other components around the accelerator, e.g. the electric insulation in the coils of quadrupoles. Estimates show an X-ray levels of  $< 10^9$  R over 20 years can keep components from failing over the linac lifetime and is con-

sidered a reasonable limit. Higher surface field cavities also need longer voltage conditioning times which may delay accelerator module production.

This concern of surface electric field has also to include the transit time factor  $T$ , which represents the effectiveness in accelerating the particles. The energy gain is proportional to  $E_0T$ . In the Upgrade design where the total length is limited, it is desirable to keep a constant energy gain for all the modules. Any drop in  $T$  has to be compensated by an increase of  $E_0$  which in turn raises the surface electric field. In other words, the important quantity for cavity design is  $E_{max}/(E_0T)$  instead of just  $E_{max}/E_0$  and in general high  $ZT^2$  and small  $E_{max}/(E_0T)$  are desired and compromises have to be made to satisfy all the criteria.

## Cavity Design

The SUPERFISH field computational program is a two dimensional program for calculating resonant frequency and fields in a rf cavity. In an SC cavity the coupling slot cannot be calculated explicitly in the program. The MAFIA<sup>[3]</sup> program can calculate three dimensional geometry, but the computer memory limits the minimum mesh size which in turn limits the accuracy. Because the coupling slot is at a position where the electric field is rather small and the size of the slot is small compared to the size of the cavity, SUPERFISH can still give satisfactory results when used in conjunction with experimental model cavities. The coupling slot is known to decrease the resonant frequency compared

to a closed cavity. The offset frequency corresponding to the cavity without coupling slot is used in the SUPERFISH calculations and is higher than the actual operational frequency (805 MHz). The amount of difference between the offset and the operational frequency depends on the coupling between the cavity and the coupling cell and is obtained through calculation and interpolation based on the experimental data from a SC model built in a collaboration effort with Los Alamos National Laboratory (LANL) and aluminum SC cavity models constructed at Fermilab<sup>[4]</sup>.

An early design for the accelerating cavity geometry along with the definition of various dimensions is shown in Fig. 1. It was derived from the LANL SC linac geometry with important modifications to be described. It is known that the frequency is not very sensitive to the size of mesh while the surface electric field is very sensitive in SUPERFISH. In a geometry where there is a large ratio in the largest and smallest dimension and using a constant mesh spacing with a limitation of  $\sim 30,000$  mesh points, there are not enough nodes around the nose cone area. This is where the electric field is changing rapidly with position so that the field distribution cannot be calculated accurately. We have modified the SUPERFISH program<sup>[5]</sup> so as to produce a mesh with a continuously varying density of nodes. With this capability we can concentrate more mesh points around the strong field region and increase the accuracy of the calculation without increasing the total mesh points and computing time.

In the process of optimizing the design the first priority and effort was given

to maximize  $ZT^2$  while trying to keep  $E_{max}/E_0$  as low as possible. The effect of varying the cavity outer radius  $R_c$ , web thickness and bore radius  $R_b$  as well as the details of the nose cone on  $ZT^2$ ,  $E_{max}/E_0$  and  $T$  have been calculated. In varying each of these dimensions, the others are kept constant while the gap distance  $G$  and related dimensions are adjusted to maintain the resonant frequency.

The dimension studied first was the cavity radius  $R_c$  which determined the overall size of the structure. The shunt impedance is most sensitive to changes in the cavity radius. Its effect on  $ZT^2$ ,  $E_{max}/E_0$  and  $T$  at 121 Mev is shown in Fig. 2.

The shunt impedance has a maximum at a certain cavity radius. This optimum cavity radius increases linearly with cell length and thus  $\beta$  ( $\beta = v/c$ , where  $v$  is the particle velocity and  $c$  the speed of light) of the particles. The cavity radius is chosen on the downhill side of the curve as close to the maximum as surface field considerations allow. Therefore a constant cavity radius throughout the energy range is not a good choice unless  $\beta$  doesn't vary greatly; otherwise either the lowest energy cavity will have a low  $ZT^2$  or the highest energy cavity will have a high  $E_{max}/E_0$ . For the Linac Upgrade the energy range of 116 Mev to 400 Mev is small enough that we choose to keep a constant cavity radius but reduce its value from the previous design value of 13.955 cm to 13.455 cm. By doing so  $ZT^2$  is increased by about 8% at the low energy end, 116 Mev, and virtually unchanged at the high energy end, 400 Mev, and

$E_{max}/(E_0T)$  is increased by about 12% and 8% respectively.

Reducing the web thickness can increase  $ZT^2$  and reduce surface field by a small amount, as shown in Fig. 3. Ultimately it is limited by the requirement of mechanical strength in the machining process and other concerns such as heat conduction from the nose cone. Because the Fermilab linac duty factor is only about 0.15%, a cooling channel is not needed in the web, and we choose to reduce the web thickness to 0.75 cm from the 1.0 cm value used in LAMPF. This raises  $ZT^2$  by about 4% at 116 Mev and about 1% at 400 Mev, and reduces the corresponding  $E_{max}/(E_0T)$  by about 1%.

The bore radius  $R_b$  turns out not to be a good dimension to change. As shown in Fig. 4, the shunt impedance drops very fast while  $E_{max}/(E_0T)$  does not or may even increase as the bore radius increases. Thus it should be determined from a beam dynamics consideration and be kept as small as possible.

## Refining the design

Historically, surface breakdown fields under cw conditions have been estimated with the empirical Kilpatrick criterion, established when untrapped oil diffusion vacuum pumps were used<sup>[6]</sup>. The criterion can be written in the form  $f = 1.643 E_k^2 \exp(-8.5/E_k)$ , where  $f$  is the frequency in MHz, and  $E_k$  is the Kilpatrick sparking limit in MV/m. The axial accelerating field  $E_0$  in a low energy standing wave structure is some fraction (typically 1/4 to 1/6) of the maximum surface field. For example, a maximum surface field of 37 MV/m

( $\simeq 5E_0$ ) for the Linac Upgrade would correspond to approximately 1.4 times the Kilpatrick limit. The present Fermilab drift-tube linac operates with a maximum surface field of about  $1 E_k$  ( $\simeq 15 \text{ MV/m}$ ) at 200 MHz.

Since no comprehensive study of maximum operating gradients exists in the literature, only power tests can ultimately determine if reliable operation is possible at the design gradient. The three constraints of conditioning time, X-ray emission and sparking rate were experimentally studied using a special 805 MHz SC power test model at Fermilab<sup>[7]</sup>. This test model was developed in collaboration with Los Alamos National Laboratory.

The SC test model has dimensions appropriate for a 200 Mev accelerating section. To obtain a statistically significant number of sparks in this short model, the ratio of the maximum surface field and average accelerating field,  $E_{max}/E_0$ , was chosen artificially high at 5.2. The maximum surface field would then be  $1.52E_k \simeq 40 \text{ MV/m}$  to reach the design gradient  $E_0 \simeq 7.6 \text{ MV/m}$  at 200 Mev. Initial results<sup>[7]</sup> from just the 6-cell portion of the model indicate that there is an initial conditioning period of about one million rf pulses (120  $\mu\text{sec}$  pulse length) during which the sparking rate drops rapidly. After this the conditioning process slows dramatically. Approximately four million rf pulses are required to bring the sparking rate down to  $5 \times 10^{-5}$  sparks/(rf pulse)/(accelerating gap) at a surface field of  $1.52 E_k$  and 120  $\mu\text{sec}$  pulse length. The sparking rate is approximately linearly proportional to the pulse length over the range of 60  $\mu\text{sec}$  to 120  $\mu\text{sec}$ . For maximum surface fields between 1.3 and 1.8  $E_k$ , the sparking

rate varies roughly like  $E_{max}^{19.5}$ .

The sparking rate achieved in the conditioned SC test model would correspond to about 1 spark/(50 rf pulses) in a complete Fermilab SC linac (448 gaps) if that cavity design were used. This is about twenty times higher than the desired sparking rate, so a considerable design effort has been made to modify the nose cone geometry where the highest fields occur. Assuming the sparking rate is proportional to the surface area and to  $E_s^{19.5}$ , the quantity of merit would thus be  $\int ds \cdot [E_s/(E_0 T)]^{19.5}$  if we want to compare nose cone geometries on the basis of the same acceleration, i.e. same  $E_0 T$ .

A double-radii nose cone<sup>[8]</sup> (Fig. 5) was adopted in order to smooth out the electric field distribution without complicating the machining. A small lower radius can help concentrate electric field close to the axis while a larger upper radius helps spread out the field distribution and reduce the peak field. A comparison of a single-radius nose cone (Fig. 5) and double-radii nose cone is given in Table 1. As can be seen the cavity with a single-radius nose cone is either more likely to spark or is less efficient in RF power.

In a double-radii nose cone the maximum surface field occurs near the tip of the nose cone and any changes that increase the radius of curvature at this point can reduce this maximum field. Three changes were considered: (1) increase the upper radius from 0.5 cm to 0.7 cm; (2) add a small straight section to the nose tip; (3) extend the upper arc of  $R_u = 0.5cm$  down another  $20^\circ$  to the  $R_l = 0.221cm$  radius arc (Fig. 5). The results are listed in Table 1. It can

be seen that the first variation is most effective in cutting down the sparking rate. The other two variations give comparable results at the low energy end, but become less effective at higher energy. In addition, calculations show the latter two options increase the high field area (the area of field within 5 to 10% of  $E_{max}$ ) by about 3 times or more of that of the first option. This increases the chance of sparking caused by imperfections introduced in the process of machining and brazing. The first variation has a predicted sparking rate at the level of 1 spark/(1000 rf pulses) for a complete linac and was chosen as the final nose cone geometry.

Finally in Fig. 6 we plotted the three important quantities,  $ZT^2$ ,  $E_{max}/E_0$  and  $T$ , of this final geometry as functions of  $\beta$  for the entire energy range concerned here.

## Summary

Looking back at what we did in the design process, we first tried to raise  $ZT^2$  by reducing cavity radius with the side effect of increasing  $E_{max}/E_0$ . We then tried to reshape the nose cone to lower  $E_{max}/E_0$  with the side effect of reducing  $ZT^2$  slightly. It is interesting to find out the overall difference between the two geometries before and after the changes, i.e. the one with  $R_c = 13.955cm$ ,  $R_n = 0.5cm$  and the other with  $R_c = 13.455cm$ ,  $R_n = 0.7cm$ , both with web thickness of  $0.75cm$ . This is done at three energies and the results are listed in Table 2.

There is an advantage with the change of the nose tip over the change in cavity radius to reduce  $E_{max}/E_0$ . In the first case the transit time factor  $T$  is changed very little because the gap distance is almost unchanged. A further calculation done at 214 Mev shows that by increasing the cavity radius to 13.755 cm without changing the nose cone, the change compared with the new geometry in  $ZT^2$  and  $E_{max}/E_0$  is little while the difference in  $T$  ( $\sim 1\%$ ) stands out. This is really a small factor and wouldn't have been a concern had the average electric field not be so high and sparking rate not be a major concern. This design is estimated to have about twice the sparking rate as the new design.

## Acknowledgements

The work described includes the contribution of many people from the Fermilab Linac Upgrade working group. The authors would like to thank in particular to T. Jurgens, Q. Kerns, T. Kroc, H.W. Miller, F. Mills, J. MacLachlan, L. Oleksiuk and D.E. Young for helpful conversations.

## References

- [1] "Fermilab Linac Upgrade Conceptual Design, Revision 3", Fermilab, July, 1989
- [2] R.K. Copper, et al, "Radio-Frequency Structure Development for the Los

Alamos/NBS Racetrack Microtron", Los Alamos Report LA-UR-83-95,  
1983

- [3] T. Weiland, et al, "MAFIA — A Three Dimensional Electromagnetic CAD system for Magnets, RF Structures, and Transient Wake-field Calculations", 1986 Linear Accelerator Conference, SLAC Report SLAC-303, 276-278, 1986
- [4] T. G. Jurgens, et al, private communication.
- [5] L. Oleksiuk, Private Communication
- [6] W. G. Kilpatrick, "Criterion for Vacuum Sparking Designed to Include Both RF and DC", Rev. Sci. Inst. 28, 824 (1957)
- [7] A. Moretti and T. Kroc, Private Communication
- [8] A suggestion of Lloyd Young, Los Alamos

## List of Tables and Figures

Table 1. Comparison of various nose designs at 121 Mev.

Table 2. Comparison of Geometries with Different  $R_c$  and  $R_u$

Fig. 1. Typical Side Coupled Cavity Geometry (805 MHz)

Fig. 2.  $ZT^2$ ,  $E_{max}/E_0$  and  $T$  vs. Cavity Radius at 165 Mev

Fig. 3.  $ZT^2$ ,  $E_{max}/E_0$  and  $T$  vs. Web Thickness at 165 Mev

Fig. 4.  $ZT^2$ ,  $E_{max}/E_0$  and  $T$  vs. Bore Radius at 165 Mev

Fig. 5. Nose Cone Shapes

Fig. 6.  $ZT^2$ ,  $E_{max}/E_0$  and  $T$  as function of  $\beta$  from 116 — 400 Mev

Table 1: Comparison of various nose designs at 121 Mev.

Nose Design	$ZT^2$		$E_{maz}/E_0$	$T$	$\Delta\{E_{maz}/(E_0T)\}^\dagger$	Relative* Sparking Rate
	( $MOhm/m$ )	$\Delta(\%)^\ddagger$			(%)	
No. 1 <sup>†</sup> ( $R_n = 0.5cm$ )	43.87	0.0	4.807	0.847	0.0	1.0
No. 1 <sup>†</sup> ( $R_n = 0.7cm$ )	42.96	-2.1	4.506	0.844	-5.9	0.23
No. 2 <sup>†</sup>	42.98	-2.0	4.380	0.844	-8.6	0.24
No. 3 <sup>†</sup>	42.95	-2.1	4.239	0.844	-11.5	0.23
No. 4 <sup>†</sup>	41.81	-4.5	4.260	0.837	-10.3	0.25

<sup>†</sup>See Fig. 5 for Nose Cone Details. Other dimensions as given in Fig.1.

<sup>‡</sup>Compared with design No. 1.

\* $\propto \int ds \cdot (\frac{B_z}{E_0T})^{19.5}$

Table 2: Comparison of Geometries with Different  $R_c$  and  $R_u$

Energy	Geometry <sup>†</sup>	$ZT^2$		$E_{max}/E_0$	$T$	$\Delta\{E_{max}/(E_0T)\}^\ddagger$	Relative*
(Mev)		(M Ohm/m)	$\Delta(\%)^\ddagger$			(%)	Sparking Rate
121	A	43.87	0.0	4.807	0.847	0.0	1.0
	B	42.96	-2.1	4.506	0.844	-5.9	0.23
	C	40.43	-7.8	4.144	0.814	-10.3	0.12
214	A	51.81	0.0	5.017	0.861	0.0	1.9
	B	50.77	-2.0	4.696	0.857	-6.0	0.41
	C	49.23	-5.0	4.464	0.830	-7.7	0.41
385	A	56.44	0.0	5.289	0.865	0.0	4.8
	B	55.32	-2.0	4.942	0.863	-6.3	0.91
	C	55.10	-2.3	4.789	0.838	-6.5	1.4

<sup>†</sup>Geometry A with  $R_c = 13.455cm$  and  $R_u = 0.5cm$ .

Geometry B with  $R_c = 13.455cm$  and  $R_u = 0.7cm$ .

Geometry C with  $R_c = 13.955cm$  and  $R_u = 0.5cm$ .

All other dimensions are the same as in Fig. 1.

<sup>‡</sup>Compared with geometry A.

\* $\propto \int ds \cdot (\frac{E_z}{E_0 T})^{19.5}$

Figure 1: Typical Side Coupled Cavity Geometry (805 MHz)

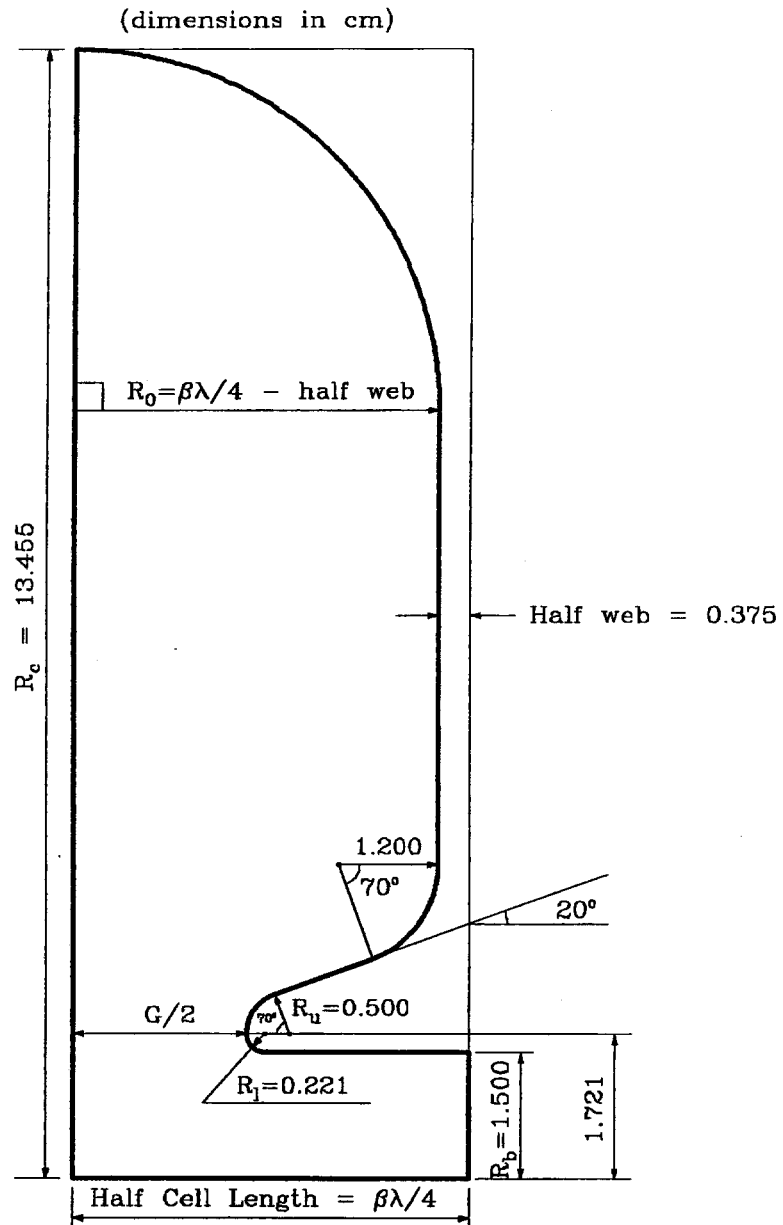


Figure 2:  $ZT^2$ ,  $E_{\max}/E_0$  and  $T$  vs. Cavity Radius at 165 Mev

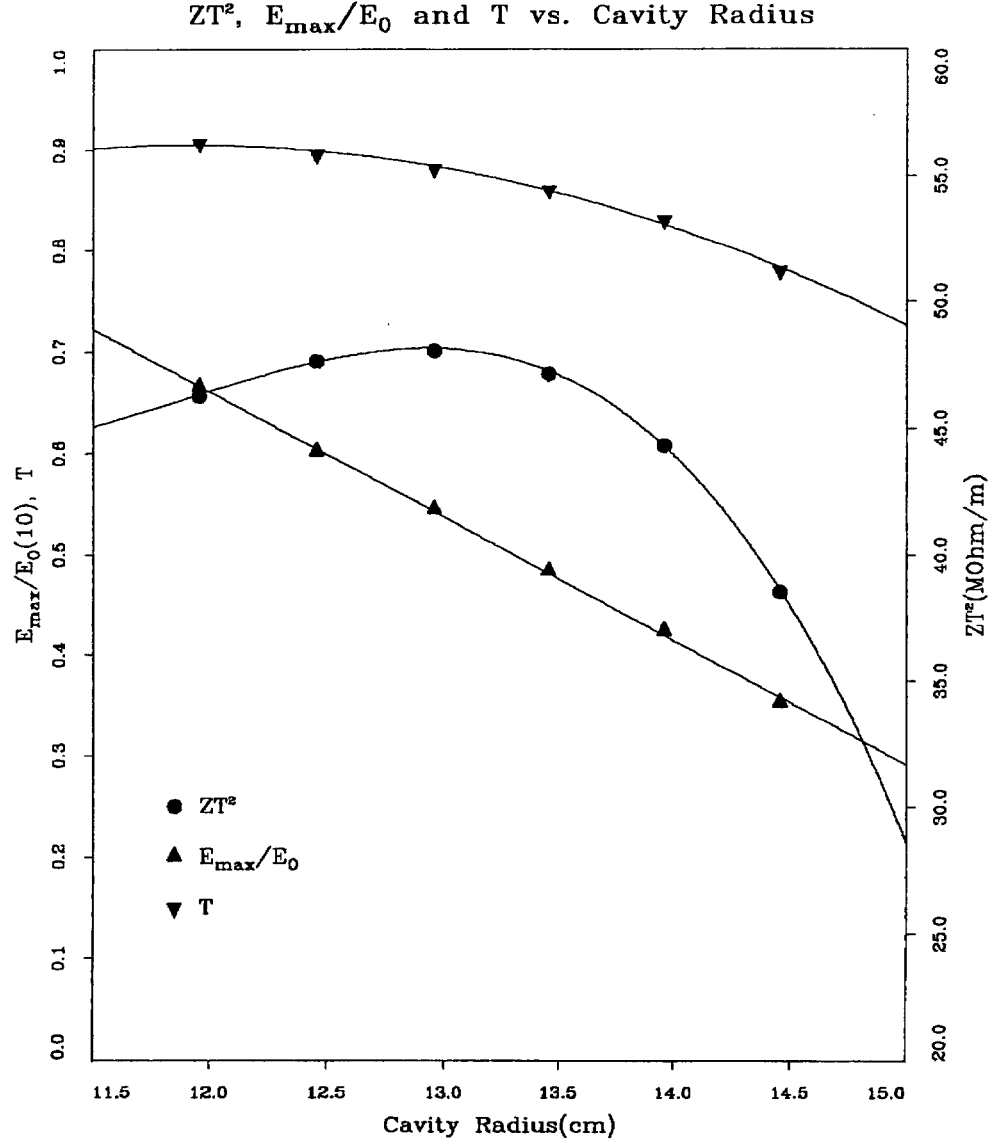


Figure 3:  $ZT^2$ ,  $E_{max}/E_0$  and  $T$  vs. Web Thickness at 165 Mev

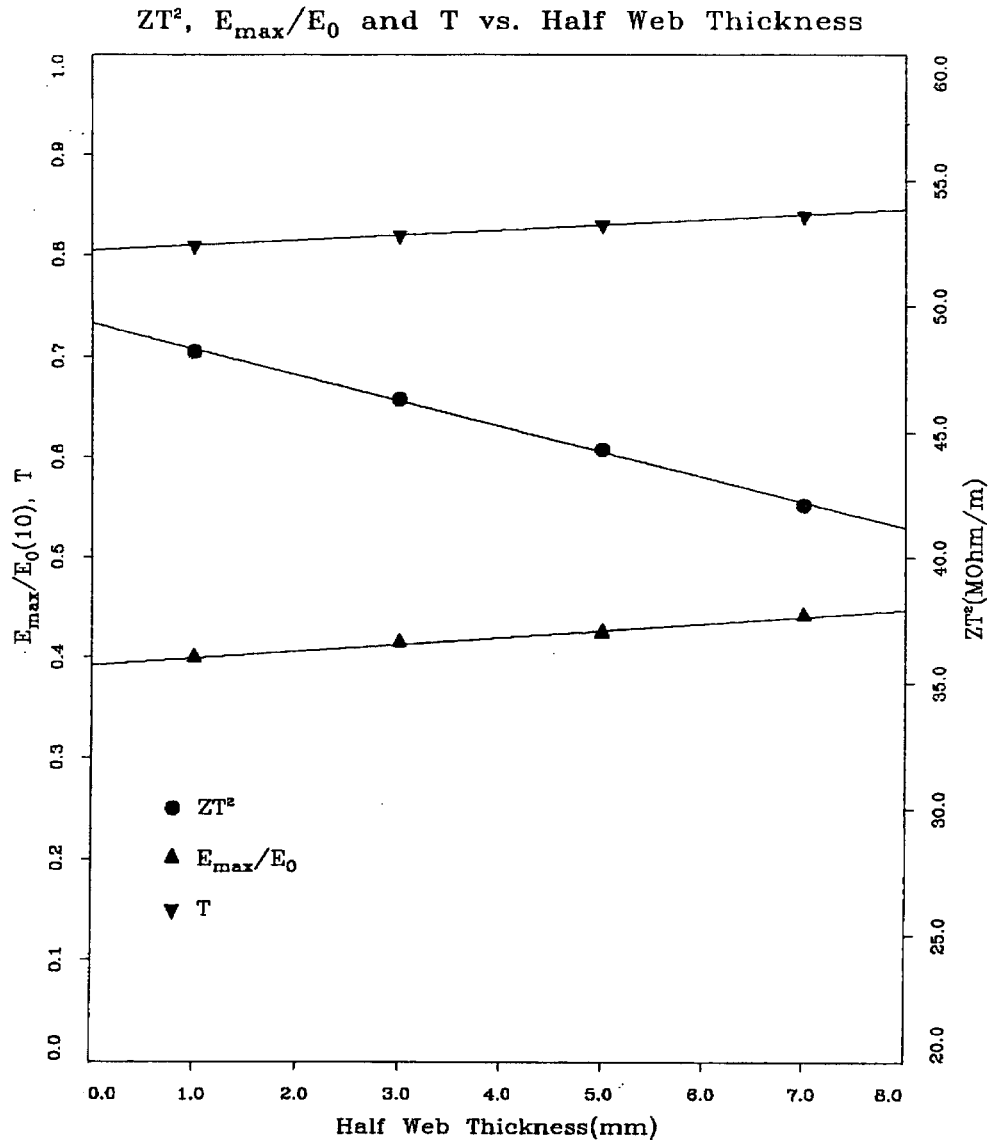


Figure 4:  $ZT^2$ ,  $E_{max}/E_0$  and  $T$  vs. Bore Radius at 165 Mev

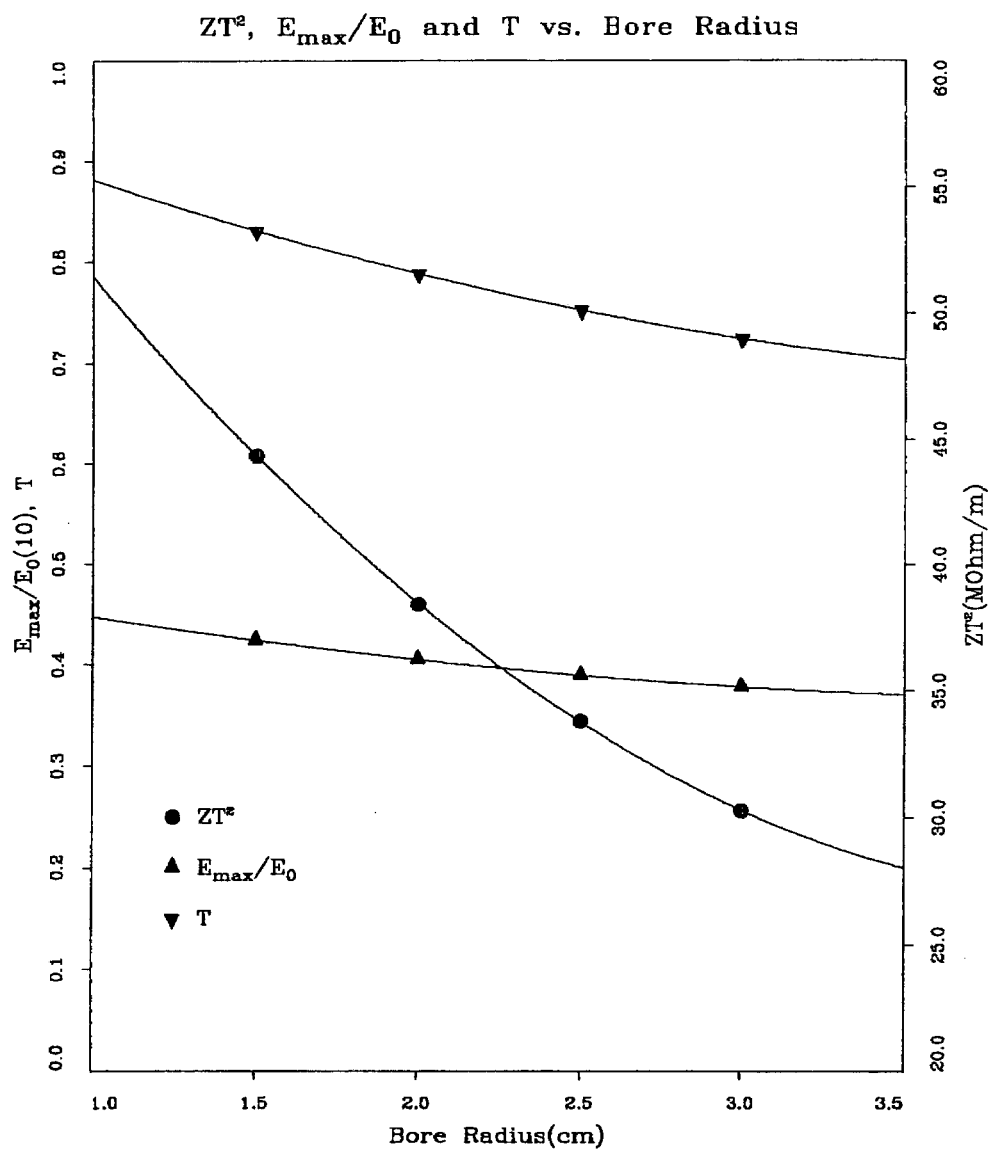


Figure 5: Nose Cone Shapes

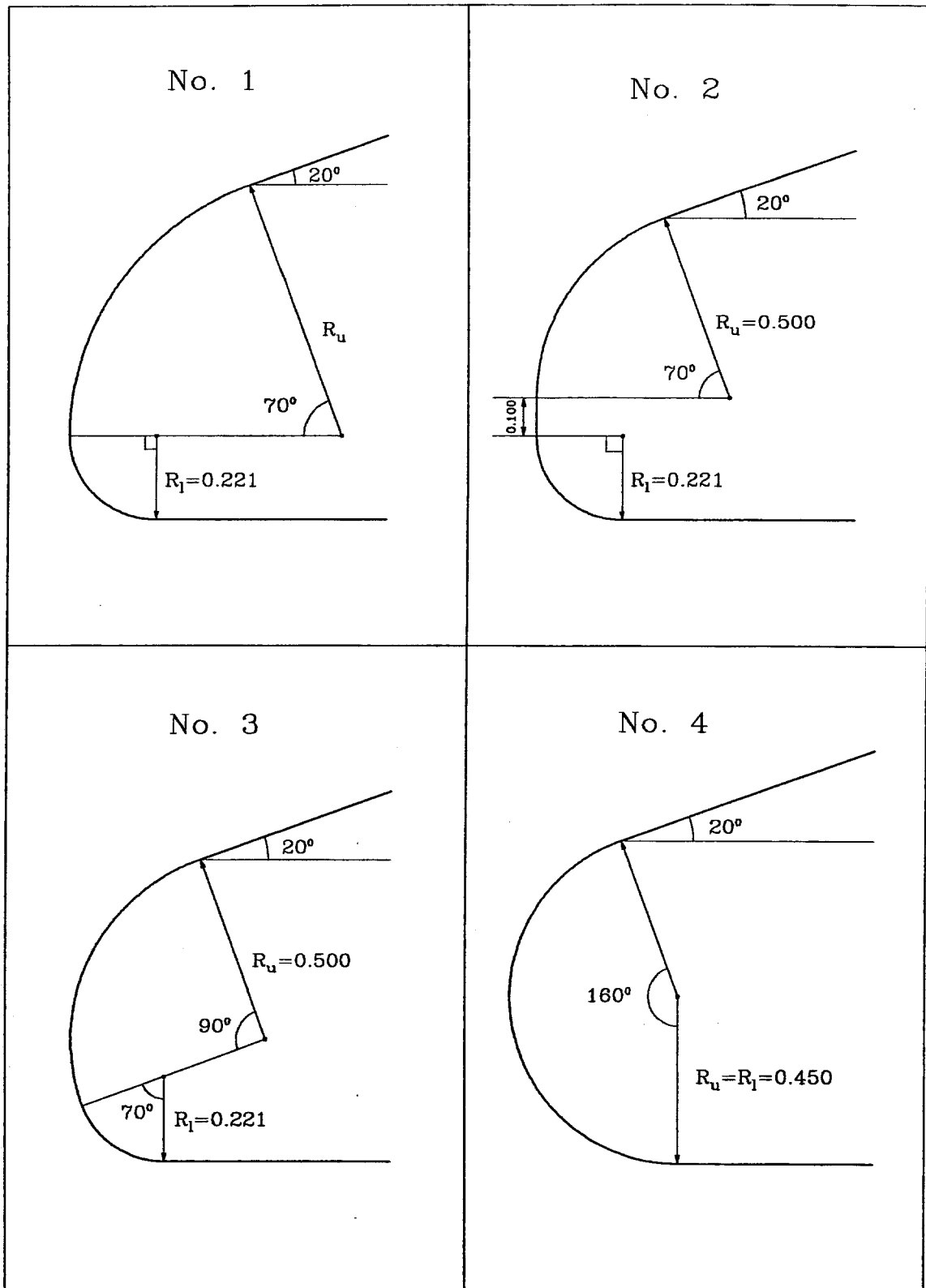


Figure 6:  $ZT^2$ ,  $E_{\max}/E_0$  and  $T$  as function of  $\beta$  from 116 — 400 Mev

